ISBN: 978-3-95450-215-8 ISSN: 2226-0366 doi:10.18429/JACoW-LINAC2022-TU1PA01

A DISCUSSION OF KEY CONCEPTS FOR THE NEXT GENERATION OF HIGH BRIGHTNESS INJECTORS

T. G. Lucas, P. Craievich, S. Reiche, Paul Scherrer Institut, 5232 Villigen PSI, Switzerland

Abstract

The production of high brightness electron beams has been key to the success of the X-ray free-electron laser (XFEL) as the new frontier in high brilliance X-ray sources. The past two decades have seen the commissioning of numerous XFEL facilities, which quickly surpassed synchrotron light sources to become the most brilliant X-ray sources. Such facilities have, so far, heavily relied on S-band RF photoguns to produce the high brightness electron bunches required for lasing, however, such photoguns are beginning to reach their performance limit. This paper aims to discuss some key ideas which are important for the development of the next generation of high brightness photoguns. A particular emphasis will be placed on the newly developing topic of intrabeam scattering which recent measurements have found to be responsible for performance limitations in a handful of injector.

INTRODUCTION

For the viability of future X-ray Free Electron Laser (XFEL) projects, it is vital for a significant improvement in the beam brightness. Current XFELs predominantly use S-band injectors which are beginning to reach the performance limit with only minor improvements possible, on paper, without a shift in technologies [1]. This limitation comes as the result of physical limits set by the intrinsic emittance in the cathode determined in part by the achievable gradient for a room temperature S-band Standing Wave (SW) Photogun. In order to make the leap to a higher brightness future, some key concepts are the focus of investigations at various labs around the world. In this paper, we aim to describe the possible benefits of moving towards two new technologies: high gradient photoguns and cold cathode technology. Each technology offers the ability to achieve a significant increase in 5D brightness. However, with these benefits there's a caveat in the form of a enhanced sliced energy spread due to intra-beam scattering (IBS). This enhanced sliced energy spread will limit the performance, particularly so in compact FELs where the beam energy is lower. These effects of IBS on the sliced energy spread require us to rethink the development of injectors for future compact FELs.

FEL PERFORMANCE AND BRIGHTNESS

Crucial to the performance of an FEL is the power generated in the lasing process. This power grows exponentially, until the amplification saturates (P_{sat}), dictated by the equation:

$$P_\gamma(s) = P_0 e^{s/L_g} < P_{sat}, \quad (1)$$

where $L_g = \frac{\lambda_u}{4\sqrt{3}\pi\rho}$ is the ideal 1D gain length. We find that this gain length is dependent on the parameter ρ, known as the 'FEL parameter' or 'Pierce parameter'. This unitless parameter is fundamental to defining several conditions of the FEL process. It can be shown, using the common definition for 5D brightness $B_{5D} \equiv 2I/\epsilon_n^2$ and ρ, that ρ has a proportionality [1]:

$$\rho \propto B_{5D}^{\frac{1}{3}}. \quad (2)$$

This is a commonly quoted proportionality in injector design and has proven to be a good figure of merit for the first generation of photoinjectors, still motivating the most recent generation of high brightness injector projects. To understand what ideas must be investigated in order to develop the next generation of high brightness photoguns, it is important to understand what limits current photoguns.

THE S-BAND ROOM-TEMPERATURE PHOTOINJECTOR

A common design of an XFEL injector consists of an S-band room temperature RF Photogun feeding a pair of S-band accelerating structures [2–4]. Table 1 details the performance of a handful of such S-band injectors. We find that each of these facilities uses very similar operational parameters particularly with a gradient between 100 and 120 MV/m. These ultimately achieves a 5D brightness in the range 200-1800 TA/m^2. Moving beyond this performance is limited by achievable gradients and the thermal emittance of the beam generated by the cathode. The following two sections will describe efforts to move beyond this 5D brightness regime through the use of high gradient photoguns and cryogenic photoguns.

HIGH GRADIENTS PHOTOGUNS

Arguably the most important development in the next generation of compact FELs is the development of high gradient technology. Along with the benefits of reducing the overall length of the linac, important for allowing the development of XFEL facilities in places with reduced space or financial means, an increase in gradient is highly beneficial to the machine brightness. In [5], it was demonstrated that the 5D brightness is proportional to:

$$B_{5D} \propto E_0^n \quad (3)$$

where E_0 is the electric field at extraction and n is between 1.5 and 2 depending on the initial bunch shape. This gives a strong motivation for moving to greater cathode gradients. Achieving a greater gradient without a significant increase in

ISBN: 978-3-95450-215-8 ISSN: 2226-0366 doi:10.18429/JACoW-LINAC2022-TU1PA01

Table 1: Performance of the current (SwissFEL, LCLS, FERMI and PAL), high gradient injector projects and a cryogenic photogun project [2, 5–9].

Parameter	SwissFEL	LCLS	FERMI	PAL	IFAST TW gun	IFAST SW gun	Overcoupled SW gun	Cryogenic S-band
Frequency (GHz)	2.998	2.856	2.998	2.856	5.712	5.712	11.7	2.856
Bunch Charge (pC)	200	250	500	250	200	200	100	200
Rep Rate (Hz)	100	120	50	60	100-400	1000	100	120
RF Pulse Length (ns)	1000	3000	3000	2000	100	300	10	900
E cath (MV/m)	100	115	120	120	135-200	160	388	240
$\epsilon_{n,slice}$ (mm mrad)	0.2	0.4	0.7	<0.3	0.2-0.155	0.2	0.1	0.05
Peak current (A)	20	45	50	80	40-60	40	25	20
B_{5D} (TA/m^2)	1000	562.5	204	1777	2000-5333	2000	5000	16000

the breakdown rate is a heavily studied topic in accelerator physics. A result which is well-established in the accelerator community is the concept that higher frequencies correlate with an ability to establish a higher peak electric field [10]. This concept was first discussed by Kilpatrick several decades ago. A more recent result comes from work performed in the domain of high gradient linear accelerators for the next generation of linear collider. Testing of several dozen travelling wave (TW) X-band accelerating structures illustrated that the breakdown rate scaled as:

$$BDR \propto E^{30}\tau^{5} \quad (4)$$

where E is the surface electric field and τ is the RF pulse length [11]. This describes how moving to shorter pulse lengths allows for an increase in surface electric field. Whether this exact relation applies to standing wave RF guns is to be established. However, this concept motivated the development of several high gradient photogun projects.

Several current projects are investigating the idea of very short fill times through either an increase in the operational frequency, a heavily overcoupled design or a shift to travelling-wave technology. As part of the IFAST high gradient photogun project, two C-band photoguns are being designed and fabricated through a collaborative effort between national laboratories and industrial partners. These RF gun are aiming for cathode gradients up to 200 MV/m through a reduced RF pulse length and doubling of the operational frequency to C-band. Taking a novel approach, one of these photoguns shifts to travelling-wave technology which allows very short fill times in comparison to its standing wave counterparts when critically-coupled. The RF design of the two guns are demonstrated in Figures 1 and 2. The parameters for these guns are illustrated in Table 1.

An extreme use of this overcoupling principle, to reduce the fill time, is found in a high gradient gun project which uses an RF pulse length of 10 ns with 3 ns flat top through an extremely overcoupled RF cavity design (Figure 2). The operational parameters of these three guns are also detailed in Table 1. These designs demonstrate that a five-fold increase in the 5D brightness, in comparison to the current SwissFEL injector, is possible. However, we will find in the final section of this paper that this is not the end of the story and such high gradient projects require further investigation on the ultimate benefits when considering performance in an FEL where sliced energy spread plays a vital role downstream of the injector in the magnetic compressor chicanes.

CRYOGENIC PHOTOGUNS

Complementing the move to higher gradients is the newly developing technology of cryogenic photoguns. The motivation for moving to a cryogenic gun comes originally from equation:

$$\epsilon_n = \sigma_x \sqrt{\frac{kT}{mc^2}} \quad (5)$$

where k is the Boltzmann constant, T is the cathode temperature and σ_x is the laser spot size on the cathode. This demonstrates a strong dependence of the 5D brightness on the internal thermal energy (kT) which comes through as the thermal emittance of the bunch on the cathode. For a cryogenic cathode with a mean temperature of 45 K, there is a reduction in the thermal emittance by a factor of 2.55, when compared to a room temperature cathode with the same spot size. This translates to a 5D brightness increase of 6.5. Such an improvement is a strong motivation for moving to cryogenic cathodes. In addition to this, recent tests of cryogenic structures have demonstrated the ability to maintain surface electric fields greater than room-temperature structures for a given breakdown rate [9]. This increase in surface electric field contributes to the brightness through the mechanism discussed in Section . Ultimately, the combined factors give a brightness increase of over an order of magnitude in comparison to current S-band room-temperature photoinjectors without the need to move to a higher frequency or shorter filling times. These factors make this concept an extremely interesting prospect in the upgrade of current XFELs.

One such cryogenic RF photogun is under development at UCLA. This cryogenic gun, when paired with an S-band TW structure (Figure 3), is predicted to achieve a normalised slice emittance of 55 nm rad which is approximately a factor of four less than that in SwissFEL. Despite no change in the peak current, the five dimensional brightness is an order of magnitude greater than current XFEL injectors systems.

INTRABEAM SCATTERING AND THE LIMITATIONS OF 5D BRIGHTNESS FOR GAUGING FEL PERFORMANCE

While both high gradients and cold cathode technologies sound like interesting prospects for future XFEL projects,

ISBN: 978-3-95450-215-8 ISSN: 2226-0366 doi:10.18429/JACoW-LINAC2022-TU1PA01

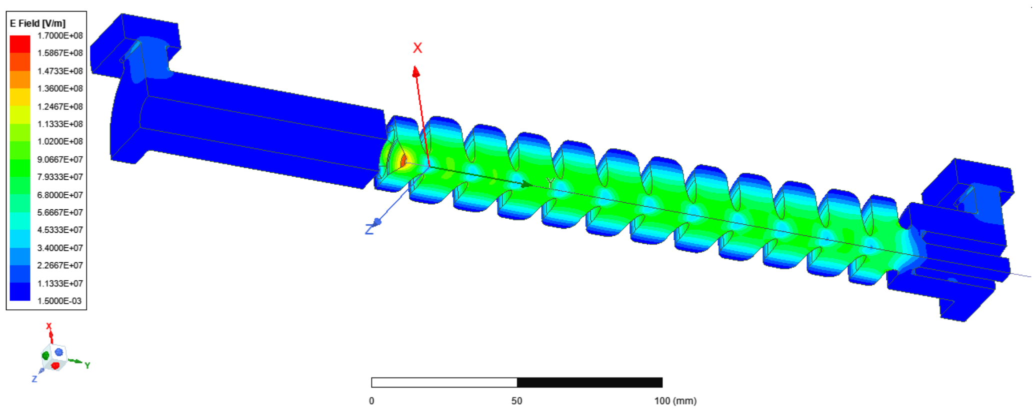

Figure 1: Electric fieldmap of the novel travelling-wave RF photogun.

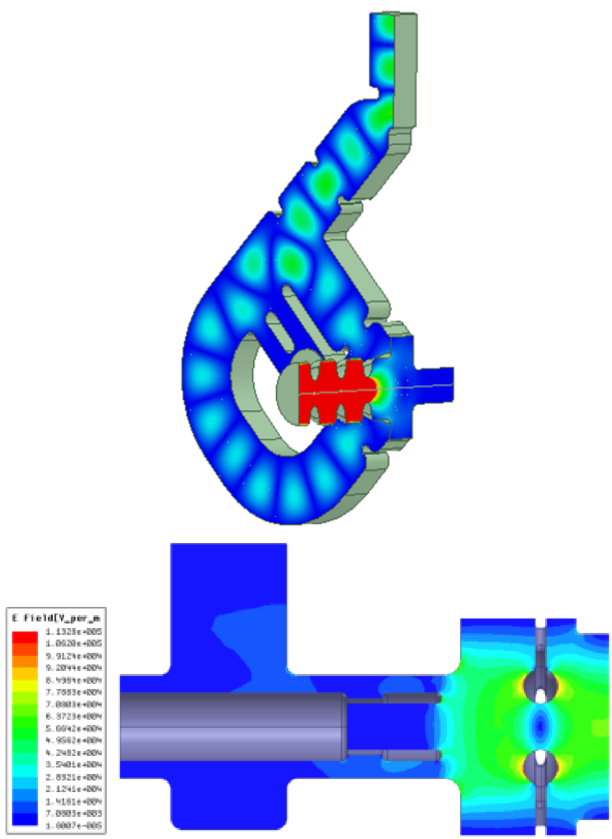

Figure 2: Two high gradient SW RF photogun projects which are underway investigating the idea of heavily overcoupled cavities [12, 13].

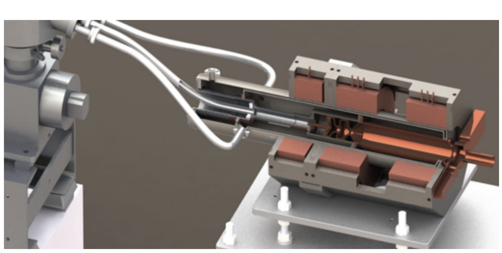

Figure 3: A rendering of the cryogenic S-band photogun [5].

recent measurements have begun to find that the classical 5D brightness, which as mentioned above is commonly used in FEL injector design, has recently begun to show signs of reaching its range of validity in FEL injector design. Measurements performed in the SwissFEL injector (Figure 4) have demonstrated a significantly greater sliced energy spread than that predicted by state-of-the-art particle tracking codes which give sliced energy spread (σ_γ) values < 1 keV [14, 15]. Such effects have also been observed in the injector of EuroXFEL and the PITZ injector [16]. The effects of this increased sliced energy spread is a limitation in compression, and the optimal compression occurs just before these sliced energy spread begin to influence the lasing. To demonstrate the effect of sliced energy spread, we first begin with the definition of the Pierce parameter:

$$\rho \equiv \frac{1}{\gamma}\left[\frac{\lambda_u^2 K^2 f_c^2}{64\pi^2}\frac{I}{I_A \sigma_x \sigma_y}\right]^{\frac{1}{3}}. \tag{6}$$

where λ_u, K and f_c are parameters which define the undulator, I is the peak current, I_A is the Alfvén current, γ is the normalised beam energy and $\sigma_{x,y}$ is the beam size. For many machines, the lattice is setup such that the sliced energy spread is on the limit of the FEL condition $\sigma_\gamma/\gamma < \rho$. By taking the case, $\sigma/\gamma \approx \rho$ and applying it to Equation 6 it can be illustrated that the Pierce parameter can be written as:

$$\rho \approx \frac{\lambda_u \lambda K^2 f_c^2}{8\pi^2 \gamma I_A}\frac{I}{\epsilon_x \epsilon_y \sigma_\gamma}. \tag{7}$$

where λ is the photon wavelength. Taking the updated definition for the pierce parameter, we find σ_γ now influences the pierce parameter when applied to an FEL with optimised compression. Defining the 6D brightness as $B_{6D} \equiv 2I/\epsilon_n^2\sigma_\gamma$ we find the proportionality:

$$\rho \propto B_{6D}. \tag{8}$$

With this we find that the accurate modelling of σ_γ is as important as the development of new technology to the development of high brightness sources for the future. In order to model the sliced energy spread accurately, the phenomena which contribute to this enhancement must be known. These

ISBN: 978-3-95450-215-8 ISSN: 2226-0366 doi:10.18429/JACoW-LINAC2022-TU1PA01

same measurements performed on the SwissFEL injector concluded that there are two phenomena contributing to the unexpectedly large σ_γ. The first of these is microbunching instabilities (MBI) in the case where these are at higher frequencies than can be resolved by longitudinal diagnostic and where they are also shoter than the cooperation length. These can then be treated as an uncorrelated energy spread source. The second phenomenon is intrabeam scattering (IBS) which had previously not been observed in an FEL injector but is well-documented in circular accelerators and similar behaviour has been documented in early vacuum tubes and monochromators [17, 18]. Here we will focus on the simulation of IBS which is of more importance to injectors.

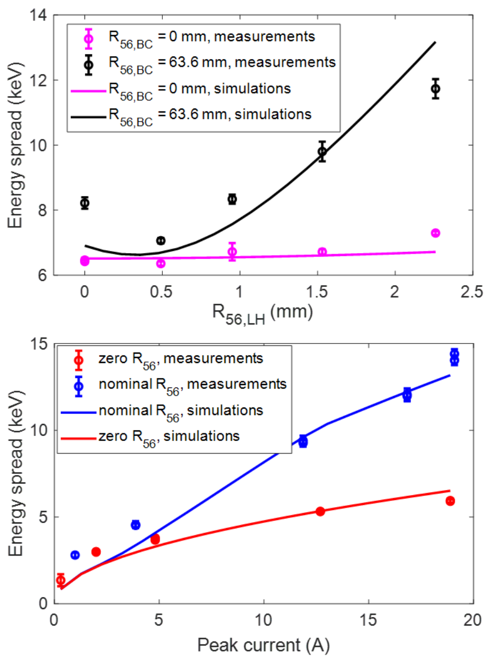

Figure 4: Sliced energy spread measurements in SwissFEL at the end of the injector for different bunch peak currents and compression levels in the bunch compressor [14].

For typical particle tracking codes such as ASTRA, GPT and OPAL, the particles are represented through macroparticles which generally represent several thousand electrons per macroparticle. Furthermore to simulate space-charge effects, the charge density of these macroparticles are assigned to a grid. These two factors lead to a filtering-out of the pair-wise interactions which are the basis of IBS. More specifically, it is difficult to describe Rutherford scattering correctly for macroparticles which have charges much higher than a single electron. A means of better describing this phenomenon, in circular machines, is found using the Piwinski equation:

$$\frac{d\sigma_\gamma^2}{dz} = \frac{2r_e N_b}{\langle\sigma_x\rangle \epsilon_x^n \sigma_z} \tag{9}$$

where r_e is the classical electron radius, N_b is the number of electrons in the bunch, $\langle\sigma_x\rangle$ is the mean transverse beam size, ϵ_x^n is the normalised emittance and σ_z is the bunch length [17, 19]. In [14], the Piwinski model was used to accurately replicate the results found in SwissFEL however with scaling factor of 2.4 on the IBS contribution to the sliced energy spread (Figure 4). This scaling factor requirement comes, in part, from momentum transfer limit imposed in the original derivation. The Piwinski equation (Equation 9) is a powerful equation and has been highly successful over the years, however, the scaling requirement illustrates that it has limitations in modelling FEL injectors. Furthermore, it also suffers from unphysical singularities for zero emittance beams where the IBS is expected to approach zero when transverse velocities approach zero. Consequently a validation of the Piwinski model is required by a different approach (e.g. through first principles by numerical simulation). In [20] it was demonstrated that a large contributor to intrabeam scattering was the waist found in the beginning of the injector between the gun and the first accelerator. Starting with the Piwinski equation, which one recalls was originally made for circular rings, one can redefine it such that it is for the case of a single waist, more appropriate for an FEL injector. This is done by setting $N_b = \sqrt{2\pi} I\sigma_z/ce$ to represent a Gaussian beam and setting the beam size (σ_x) which follows a waist equation defined as:

$$\sigma(z) = \sigma_0\sqrt{1+\frac{z^2}{\beta_0^2}} \tag{10}$$

where β_0 is the betatron function at the waist. This gives us a reformulated Piwinski equation for a waist:

$$\sigma_\gamma^2 = \sqrt{8\pi}\frac{r_e^2}{ce}\frac{I\sigma_0\gamma}{\epsilon_n^2}\int_{-\infty}^{\infty}\frac{d\hat{z}}{\sqrt{1+\hat{z}^2}}. \tag{11}$$

where $\hat{z} = z/\beta_0$ is the z position normalised to the betatron function at the waist. Although this concept is a more accurate depiction of FEL injectors, Equation 11 still has a singularity for zero emittance and also has a logarithmically divergent integral. These factors mean that a new modelling method must be sort to accurately model IBS behaviour over a wider range of beam parameters.

One route to the modelling of IBS is through the use of numerical codes such as GPT and OPAL which offer an additional space-charge model based on pair-wise space-charge interactions. This allows the electron scattering process to be modelled in the situation where each macroparticle represents a single electron. The limitation of this technique is the computational power requirements, where the calculation time scales as N^2, where N is the number of macroparticles. This limitation means that the modelling bunch charges in excess of 1 pC is time-intensive given current computation power. Despite this, such a model can be useful for understanding the dependence of IBS on various beam parameters. Using the GPT particle tracking package, a 50 fC bunch was defined externally and imported into the GPT code before being tracked through a waist with a given β where the start of the waist was set to values large enough where IBS-induced sliced energy spread increases were not visible above the

ISBN: 978-3-95450-215-8 ISSN: 2226-0366 doi:10.18429/JACoW-LINAC2022-TU1PA01

simulation noise. This was performed numerous times in a Monte Carlo style simulation to account for large angle scattering events which add large fluctuations in the value of the energy spread for an individual run. Figure 5 demonstrates the sliced energy spread increase when a beam passes through a waist given a set of initial beam parameters. Each point represents the median value of sliced energy spread increase for 100 iterations of the same simulation, with randomised initial particle distributions. These simulations found the dependence:

$$\sigma_\gamma \propto \frac{\gamma^{0.38} I^{0.46} \sigma_0^{0.32}}{\epsilon_n^{0.63}}. \tag{12}$$

Such exponents were fitted over a limited range of simulation parameters and these values may change based on this range. A particular case we expect is when the emittance approaches zero. During these scans the remaining parameters remained constant with a geometric emittance (ϵ_x) of 1 nm rad, an energy (γ) of 20, a minimum waist (σ_0) of 3 μm and a peak current of 2 mA. These results are found to be similar to those of the rederived Piwinski equation for a waist, however for the numerical model, one can determine the dependence for different regimes which may become unphysical in the analytical solution, such as for very low emittance in ultra-cold beams. These numerical simulations represent early results in the modelling this phenomenon correctly and the authors predict significant work will be required for an accurate model to be developed.

CONCLUSIONS

The past two decades have seen the successful commissioning of several XFELs which now serve dozens of user stations with the highest brightness X-ray beams available. In order to continue the development of XFELs to further increase beam brightness, one must continue the development of photoinjectors. The current solution of a room-temperature S-band photoinjector is reaching its performance limit primarily determined by the achievable cathode gradient and thermal emittance on the cathode. The next generation of photoinjectors for compact XFELs should aim to move to higher cathode gradients in order to increase 5D brightness possibly with the addition of cold cathode technology. However, recent measurements of sliced energy spread suggest that the shift to better FEL performance may not be as straight forward as increasing 5D brightness. The accurate modelling of intrabeam scattering will be vital for determining the beam quality available. Modelling IBS using the Piwinski equation provides better results than current particle tracking codes however it still does not accurately predict IBS in FEL injectors. A new means of modelling IBS using numerical codes is under investigation and appears to provide results consistant with a reformulated Piwinski equation for a waist whilst also not suffering from divergent integrals and singularities as found in the analytical equation. Further investigations into how to model this phenomenon are ongoing and will be key to a high brightness upgrade for future XFELs.

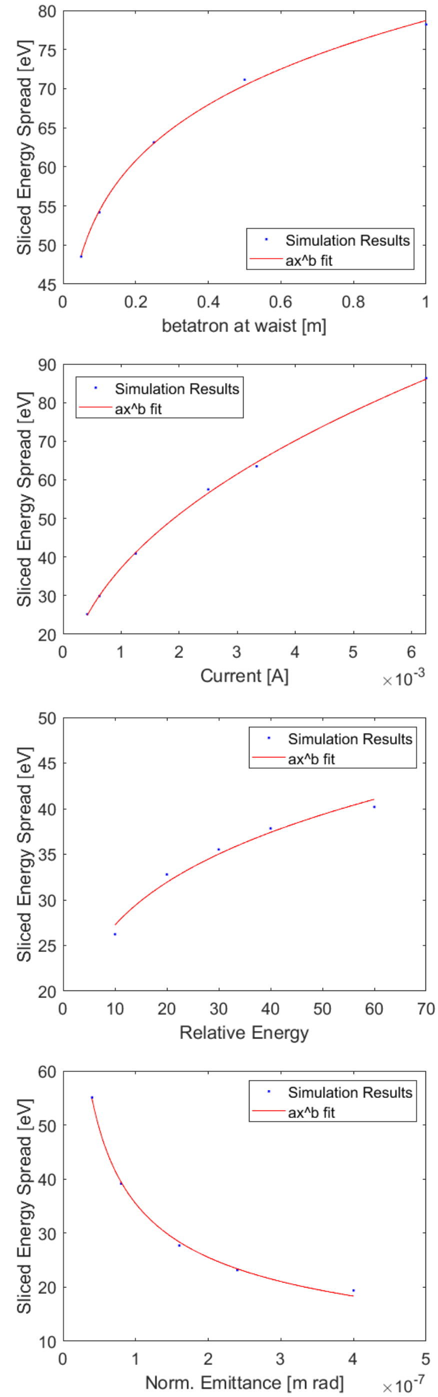

Figure 5: Parameter scan of certain beam parameters to find the dependence of sliced energy spread through a waist.

ACKNOWLEDGEMENTS

The authors would sincerely like to thank the each of the labs which have contributed operational parameters of their machines.

ISBN: 978-3-95450-215-8 ISSN: 2226-0366 doi:10.18429/JACoW-LINAC2022-TU1PA01

FUNDING

This project has received funding from the European Union's Horizon 2020 Research and Innovation program under GA No101004730.

REFERENCES

[1] M. Schaer, "RF traveling-wave electron gun for high brightness", PhD Thesis, ETH Zurich, Switzerland, 2016. doi:10.3929/ethz-a-010749949

[2] J. H. Han *et al.*, "Beam operation of the PAL-XFEL Injector Test Facility", in *Proc. FEL'14*, Basel, Switzerland, Aug. 2014, paper WEB02, pp. 615–622.

[3] T. Schietinger *et al.*, "Commissioning experience and beam physics measurements at the SwissFEL Injector Test Facility", *Phys. Rev. Accel. Beams*, vol. 19, p. 100702, 2016. doi:10.1103/PhysRevAccelBeams.19.100702

[4] P. Emma *et al.*, "Initial commissioning experience with the LCLS injector", in *Proc. PAC'07*, Albuquerque, NM, USA, Jun. 2007, paper TUPMS049, pp. 1302–1304.

[5] J. B. Rosenzweig, "Next generation high brightness electron beams from ultrahigh field cryogenic rf photocathode sources", *Phys. Rev. Accel. Beams*, vol. 22, p. 023403. doi:10.1103/PhysRevAccelBeams.22.023403

[6] Feng Zhou, private communication.

[7] Mauro Trovo, private communication.

[8] Chang-Ki Min and Jang-Hui Han, private communication.

[9] A. D. Cahill, J. B. Rosenzweig, V. A. Dolgashev, S. G. Tantawi, and S. Weathersby "High gradient experiments with X-band cryogenic copper accelerating cavities", *Phys. Rev. Accel. Beams*, vol. 21, p. 102002, 2018. doi:10.1103/PhysRevAccelBeams.21.102002

[10] W. D. Kilpatrick, "Criterion for vacuum sparking designed to include both rf and dc", *Rev. Sci. Instrum.*, vol. 28, p. 824, 1957. doi:10.1063/1.1715731

[11] A. Grudiev, S. Calatroni, and W. Wuensch, "New local field quantity describing the high gradient limit of accelerating structures", *Phys. Rev. ST Accel. Beams*, vol. 12, p. 102001, 2009. doi:10.1103/PhysRevSTAB.12.102001

[12] D. Alesini *et al.*, "The new C band gun for the next generation RF photo-injectors", in *Proc. IPAC'22*, Bangkok, Thailand, Jun. 2022, pp. 679–682. doi:10.18429/JACoW-IPAC2022-MOPOMS021

[13] C. Jing, "The first beam of an ultrahigh gradient RF photogun", presented at the Snowmass'21 Electron Source Workshop, Feb. 2022. https://indico.fnal.gov/event/46053/contributions/232504/

[14] E. Prat *et al.*, "Energy spread blow-up by intra-beam scattering and microbunching at the SwissFEL injector", presented at the FEL'22, Trieste, Italy, Aug. 2022, paper WEB03.

[15] E. Prat, P. Dijkstal, E. Ferrari, A. Malyzhenkov, and S. Reiche, "High-resolution dispersion-based measurement of the electron beam energy spread", *Phys. Rev. Accel. Beams*, vol. 23, p. 090701, 2020. doi:10.1103/PhysRevAccelBeams.23.090701

[16] S. Tomin, I. Zagorodnov, W. Decking, N. Golubeva, and M. Scholz, "Accurate measurement of uncorrelated energy spread in electron beam", *Phys. Rev. Accel. Beams*, vol. 24, p. 064201, 2021. doi:10.1103/PhysRevAccelBeams.24.064201

[17] A. Piwinski, "Intra-beam scattering", in *Proc. 9th Int. Conf. on High Energy Accelerators*, SLAC, Stanford, CA, USA, May, 1974, pp. 405–409. doi:10.5170/CERN-1992-001.226

[18] P. C. Tiemeijer, "Measurement of Coulomb interactions in an electron beam monochromator", *Ultramicroscopy*, vol. 78, pp. 53–62, 1999. doi:10.1016/S0304-3991(99)00027-3

[19] Z Huang, "Intrabeam xcattering in an X-ray FEL driver", SLAC, Stanford, CA, USA, Rep. LCLS-TN-02-8, Nov. 2002.

[20] R. Robles, "Versatile, high brightness, cryogenic photoinjector electron source", *Phys. Rev. Accel. Beams*, vol. 24, p. 063401. doi:10.1103/PhysRevAccelBeams.24.063401